Published OnlineFirst January 6, 2015; DOI: 10.1158/2159-8290.CD-14-1326

RESEARCH BRIEF

Lysine Demethylase KDM4A Associates with Translation Machinery and Regulates Protein Synthesis

Capucine Van Rechem[1], Joshua C. Black[1], Myriam Boukhali[1], Martin J. Aryee[2], Susanne Gräslund[3], Wilhelm Haas[1], Cyril H. Benes[1], and Johnathan R. Whetstine[1]

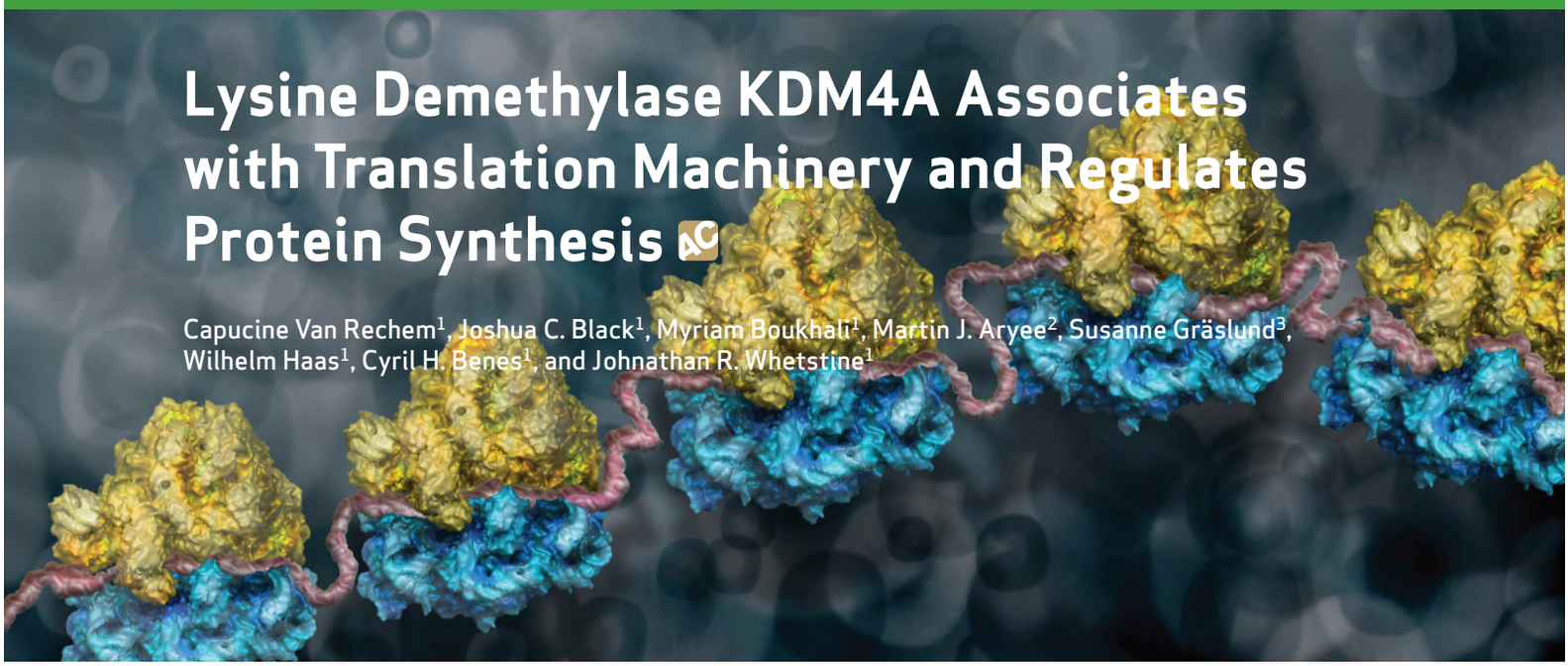

ABSTRACT Chromatin-modifying enzymes are predominantly nuclear; however, these factors are also localized to the cytoplasm, and very little is known about their role in this compartment. In this report, we reveal a non–chromatin-linked role for the lysine-specific demethylase KDM4A. We demonstrate that KDM4A interacts with the translation initiation complex and affects the distribution of translation initiation factors within polysome fractions. Furthermore, KDM4A depletion reduced protein synthesis and enhanced the protein synthesis suppression observed with mTOR inhibitors, which paralleled an increased sensitivity to these drugs. Finally, we demonstrate that JIB-04, a JmjC demethylase inhibitor, suppresses translation initiation and enhances mTOR inhibitor sensitivity. These data highlight an unexpected cytoplasmic role for KDM4A in regulating protein synthesis and suggest novel potential therapeutic applications for this class of enzyme.

SIGNIFICANCE: This report documents an unexpected cytoplasmic role for the lysine demethylase KDM4A. We demonstrate that KDM4A interacts with the translation initiation machinery, regulates protein synthesis and, upon coinhibition with mTOR inhibitors, enhances the translation suppression and cell sensitivity to these therapeutics. *Cancer Discov; 5(3); 255–63. ©2015 AACR.*

See related commentary by Rothbart et al., p. 228.

See related article by Van Rechem et al., p. 245.

INTRODUCTION

Although sites of lysine methylation are emerging for non-histone substrates, little is known about how the enzymes responsible for the addition and removal of methylation, lysine methyltransferases (KMT) and lysine demethylases (KDM), respectively, are affecting the associated targets or their downstream processes. Most studies are focused on how these enzymes are targeting nuclear proteins, even though there are important roles outside the nucleus (1–3). Therefore, studying the functions of KMTs and KDMs in the cytoplasmic compartment could reveal unexpected roles,

[1]Massachusetts General Hospital Cancer Center and Department of Medicine, Harvard Medical School, Charlestown, Massachusetts. [2]Massachusetts General Hospital Department of Pathology and Department of Medicine, Harvard Medical School, Charlestown, Massachusetts. [3]Structural Genomics Consortium, University of Toronto, Toronto, Ontario, Canada.

Note: Supplementary data for this article are available at Cancer Discovery Online (http://cancerdiscovery.aacrjournals.org/).

Corresponding Author: Johnathan R. Whetstine, Department of Medicine, Massachusetts General Hospital Cancer Center, Harvard Medical School, Building 149, Room 7-213, 13th Street, Charlestown, MA 02129. Phone: 617-643-4347; Fax: 617-724-9648; E-mail: jwhetstine@hms.harvard.edu

doi: 10.1158/2159-8290.CD-14-1326

Published OnlineFirst January 6, 2015; DOI: 10.1158/2159-8290.CD-14-1326

which will likely identify relationships between these enzymes and signaling pathways (1). Understanding the nuclear and cytoplasmic roles for these chromatin-modifying enzymes is important because they are commonly altered in cancer (4), affect numerous diseases (5), and are emerging as important therapeutic targets.

In this study, we describe a new and unexpected cytoplasmic role for the lysine demethylase KDM4A. KDM4A is a JmjC domain–containing enzyme that demethylates H3K9me3, H3K36me3, and H1.4K26me3 (6). Previous studies have documented roles for KDM4A in modulating DNA replication, site-specific copy-number regulation, and gene expression (7–9). These functions relate to the nuclear role of KDM4A; however, KDM4A is also localized to the cytoplasm, suggesting non–chromatin-mediated functions. We report that KDM4A interacts with the translation initiation factors and is present in the initiating fractions of polysome profiles. Consistent with these observations, KDM4A depletion altered the distribution of translation initiation factors in polysome profiles, reduced protein synthesis, and enhanced the cell sensitivity and effect of mTOR inhibitors. Finally, we demonstrate that chemical inhibition with JIB-04, a JmjC demethylase inhibitor, potently inhibits translation initiation, reduces overall translation, and enhances mTOR inhibitor sensitivity. Taken together, the findings in this report reveal an unexpected direct interaction between KDM4A and components of the translation machinery and highlight KDM4A as well as other JmjC proteins as potentially new targets in combined cancer therapy.

RESULTS

KDM4A Interacts with the Translation Initiation Machinery

The lysine demethylase KDM4A is located in both the nucleus and cytoplasm (Fig. 1A). For this reason, we performed mass spectrometry analysis on endogenously immunoprecipitated KDM4A from whole-cell extracts to identify interacting proteins from both compartments. The interacting proteins from two independent immunoprecipitations were analyzed by Ingenuity Pathway Analysis (IPA), which revealed a significant enrichment for proteins involved in translation ($P = 1.74E{-}13$ and $2.58E{-}14$, respectively; Fig. 1B). We further confirmed these interactions with a separate KDM4A antibody by conducting coimmunoprecipitations (Fig. 1C). Some of these associations were equal to, or more enriched than, previously confirmed KDM4A interactors (e.g., compare eIF2α with MCM-7 or P53; refs. 8, 10). We further strengthened these observations by isolating fractions from polysome profiles and Western blotting for KDM4A and associated proteins as well as for positive controls for the collections. KDM4A was enriched in the translation-initiating fractions: predominantly in the 40S fractions and, to a lesser extent, in the 60S fractions (Fig. 1D; fractions 5–9). These data suggest that KDM4A could directly affect translation.

KDM4A Affects Initiation Factor Distribution in the 40S, 60S, and 80S Fractions

To understand the impact that KDM4A could have on the translation machinery, we siRNA-depleted KDM4A and assessed whether the protein levels of translation-related factors were altered using multiplexed quantitative mass spectrometry–based proteomics (11). We compared the proteome of unaltered and KDM4A-depleted cells in biologic duplicates. The protein levels of more than 8,200 individual proteins were quantified. We did not observe changes in levels for translation-related factors. In fact, proteins that are upregulated (19 proteins greater than 1.7-fold) and downregulated (four proteins decreased by 1.7-fold; Supplementary Fig. S1A) did not have a significant enrichment in any particular category by IPA analysis ($P < 0.05$). We observed only four proteins that were downregulated by more than 1.7-fold upon KDM4A depletion, including KDM4A (Supplementary Fig. S1A). Consistent with our quantitative proteomics data, Western blotting confirmed the absence of major differences in translation-related protein levels (Supplementary Fig. S1B).

Because KDM4A was present in the initiating fractions within the polysome profile, we assessed the impact KDM4A depletion had on initiation factor levels and distribution within the polysome fractions. KDM4A depletion resulted in the enrichment of initiation factors in certain fractions (i.e., 40S) and/or a redistribution of these factors such that there was an extension into larger fractions (i.e., 60S and 80S; Fig. 2A and Supplementary Fig. S1C). Figure 2A depicts the average change across two independent siRNA-treated samples. The red bars highlight fractions with >20% change in protein levels for both independent siRNAs. We consistently observed an increase in eIF3A, FXR1, eIF4A1, eIF2α, and eIF5A protein levels in some of their corresponding fractions across two independent KDM4A siRNAs (see representative Western blot analyses and red bars in accompanying graphs), whereas eIF3A, FXR1, and eIF2α presence is extended in larger fractions (fractions 11, 7, and 7–8, respectively). eIF5A is consistently enriched in fractions 5–6 upon KDM4A depletion, whereas PABP is stable across all fractions and serves as a normalization control.

We further investigated the impact that KDM4A had on initiation factor distribution by overexpressing enzymatically active and inactive KDM4A. We compared the distribution of translation factors in cells expressing GFP alone (GFP), catalytically active KDM4A (GFP-WT), or catalytically inactive KDM4A (GFP-H188A; ref. 7). For both GFP-WT and GFP-H188A, the distribution of initiation factors was altered. For example, eIF3A, FXR1, and eIF4A1 protein levels were consistently higher in fractions 6–11 (Fig. 2B and Supplementary Fig. S1D; red bars, >20% between independent experiments). GFP-H188A appeared to have a more pronounced effect on certain initiation factors (i.e., eIF3A was higher in fractions 8–9 and FXR1 was increased in fractions 6–10). Interestingly, whereas GFP-WT and GFP-H188A had comparable expression (Fig. 2B, top), GFP-H188A exhibited much higher levels in fractions 5–9 (Fig. 2C). These data are consistent with the catalytic activity being important for KDM4A distribution within the initiating fractions. Taken together, these data highlight the importance of balancing KDM4A protein levels so that proper distribution of translation initiation factors occurs within polysome profiles, which supports a role for KDM4A in initiation complex assembly/disassembly (Fig. 2D).

KDM4A Depletion Reduces Protein Synthesis

Because KDM4A interacts with translation factors and affects their distribution, we hypothesized that KDM4A

Published OnlineFirst January 6, 2015; DOI: 10.1158/2159-8290.CD-14-1326

A

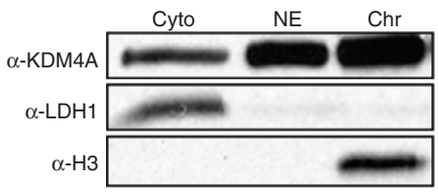

B

	Set 1			Set 2		
	KDM4A	IgG	NSAF	KDM4A	IgG	NSAF
KDM4A	212	0	7.2E–03	219	0	9.0E–03
MCM3	0	0		16	0	8.8E–04
MCM5	0	0		3	0	1.8E–04
RFC1	6	0	1.9E–04	2	0	7.8E–05
SSBP1	3	0	1.9E–04	2	2	5.9E–04
ABCF1	4	0	1.7E–04	5	0	2.6E–04
CKAP5	2	0	3.6E–05	0	0	
CNBP	4	0	8.6E–04	0	0	
DHX9	105	24	3.0E–03	74	10	2.6E–03
EEF1A1	0	0		11	5	1.1E–03
EEF2	0	0		13	5	6.8E–04
EIF2S1	2	0	2.3E–04	0	0	
EIF3D	5	0	3.2E–04	2	0	1.6E–04
EIF4A1	0	0		2	0	2.2E–04
EIF4A3	0	0		6	0	6.4E–04
EIF4G1	15	0	3.5E–04	7	0	2.0E–04
EMR1	0	0		6	0	4.2E–04
FN1	6	0	9.3E–05	21	0	4.0E–04
FXR1	7	0	4.1E–04	8	0	5.7E–04
GNB2L1	7	2	8.2E–04	0	0	
HNRNPK	29	10	2.3E–03	12	0	1.2E–03
HSPA5	0	0		11	6	7.6E–04
IGF2BP1	16	0	1.0E–03	13	0	1.0E–03
IGF2BP3	0	0		9	0	7.0E–04
MRPL15	2	0	2.5E–04	0	0	
NCBP1	3	0	1.3E–04	0	0	
NCBP2	4	0	9.1E–04	0	0	
NCL	62	32	3.3E–03	32	0	2.1E–03
PABPC4	33	4	1.9E–03	24	0	1.7E–03
PTBP1	23	7	1.6E–03	8	0	7.0E–04
RPL17	16	0	3.1E–03	10	2	2.4E–03
RPL23	20	6	5.5E–03	19	5	6.3E–03
RPL24	9	3	2.0E–03	8	0	2.2E–03
RPL27A	15	0	3.6E–03	10	0	2.9E–03
RPS14	25	7	6.4E–03	30	8	9.4E–03
RPS29	3	0	1.8E–03	0	0	
RPS3	32	14	6.3E–04	20	7	6.0E–03
RPS3A	42	11	5.7E–03	36	14	6.0E–03
RPS4X	54	17	7.4E–03	28	3	4.7E–03
RPS6	17	0	2.4E–03	10	0	1.7E–03
RPS9	21	0	3.7E–03	19	0	4.1E–03
RRBP1	15	0	4.0E–03	3	0	9.9E–05
UPF1	20	0	6.6E–04	17	0	6.9E–04
IPA *P* value	1.74E–13			2.58E–14		

C

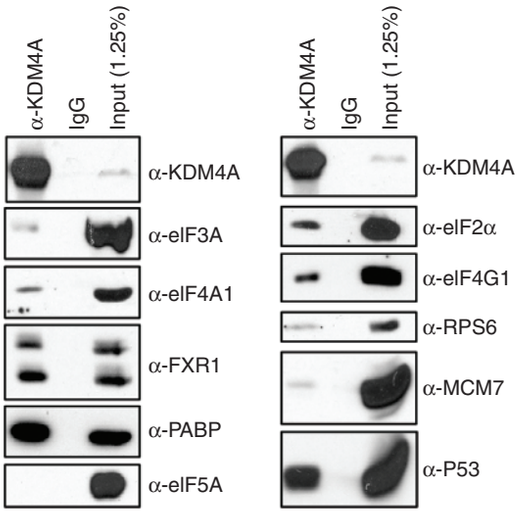

D

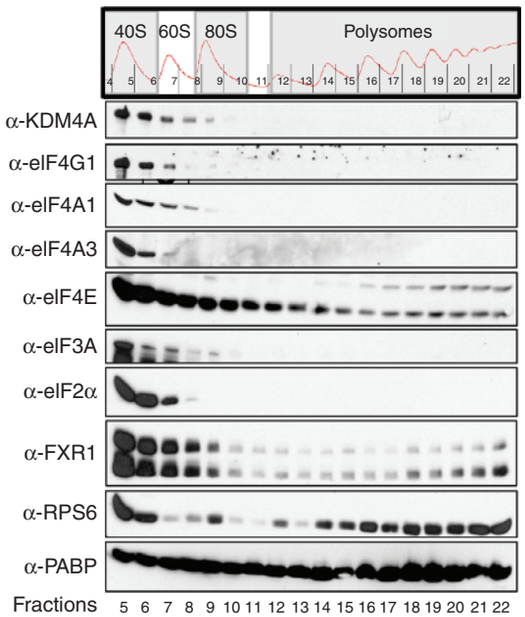

Figure 1. KDM4A interacts with the translation initiation machinery. **A,** KDM4A is present in the cytoplasm and the nucleus. RPE cells were fractionated and Western blotted for KDM4A and control proteins for the fractionations. **B,** KDM4A interacts with the translation initiation machinery. Endogenous KDM4A was immunoprecipitated with a rabbit polyclonal antibody from HEK 293T cells and analyzed by mass spectrometry. The upper part of the table (in color; ref. 8) represents the peptides and Normalized Spectral Abundance Factor (NSAF) values for KDM4A and previously confirmed interactors. The bottom part of the table (in white) represents the proteins present in the IPA "translation" category. **C,** KDM4A interacts with the translation initiation machinery. These interactions were confirmed by Western blotting Fab-immunoprecipitated KDM4A from HEK 293T cells. **D,** KDM4A sediments in the 40S and 60S polysome fractions. HEK 293T lysates were separated on sucrose gradient before fractions from polysome profiles were collected and immunoblotted with the indicated antibodies.

would have a role in protein synthesis. To test this possibility, we depleted KDM4A with two different shRNAs and assessed protein synthesis over 2 hours by measuring the incorporation of the methionine analogue AHA (L-azidohomoalanine; Fig. 3A and Supplementary Fig. S2A). KDM4A depletion significantly reduced the synthesis of nascent proteins (Fig. 3A; 40%; $P = 1E{-}05$).

We then assessed whether KDM4A depletion could enhance the inhibition of protein synthesis caused by drugs targeting translation initiation. mTOR is a well-recognized drug target involved in translation initiation (12, 13). Therefore, we depleted KDM4A and assessed AHA incorporation with increasing doses of the mTOR inhibitor rapamycin. Protein synthesis was further decreased in cells treated with all doses of rapamycin combined with *KDM4A* shRNA depletion (Fig. 3B and Supplementary Fig. S2B). For example, 0.1 and 1 ng/mL rapamycin suppressed protein synthesis by approximately 20% and 50%, respectively. However, 0.1 ng/mL

Published OnlineFirst January 6, 2015; DOI: 10.1158/2159-8290.CD-14-1326

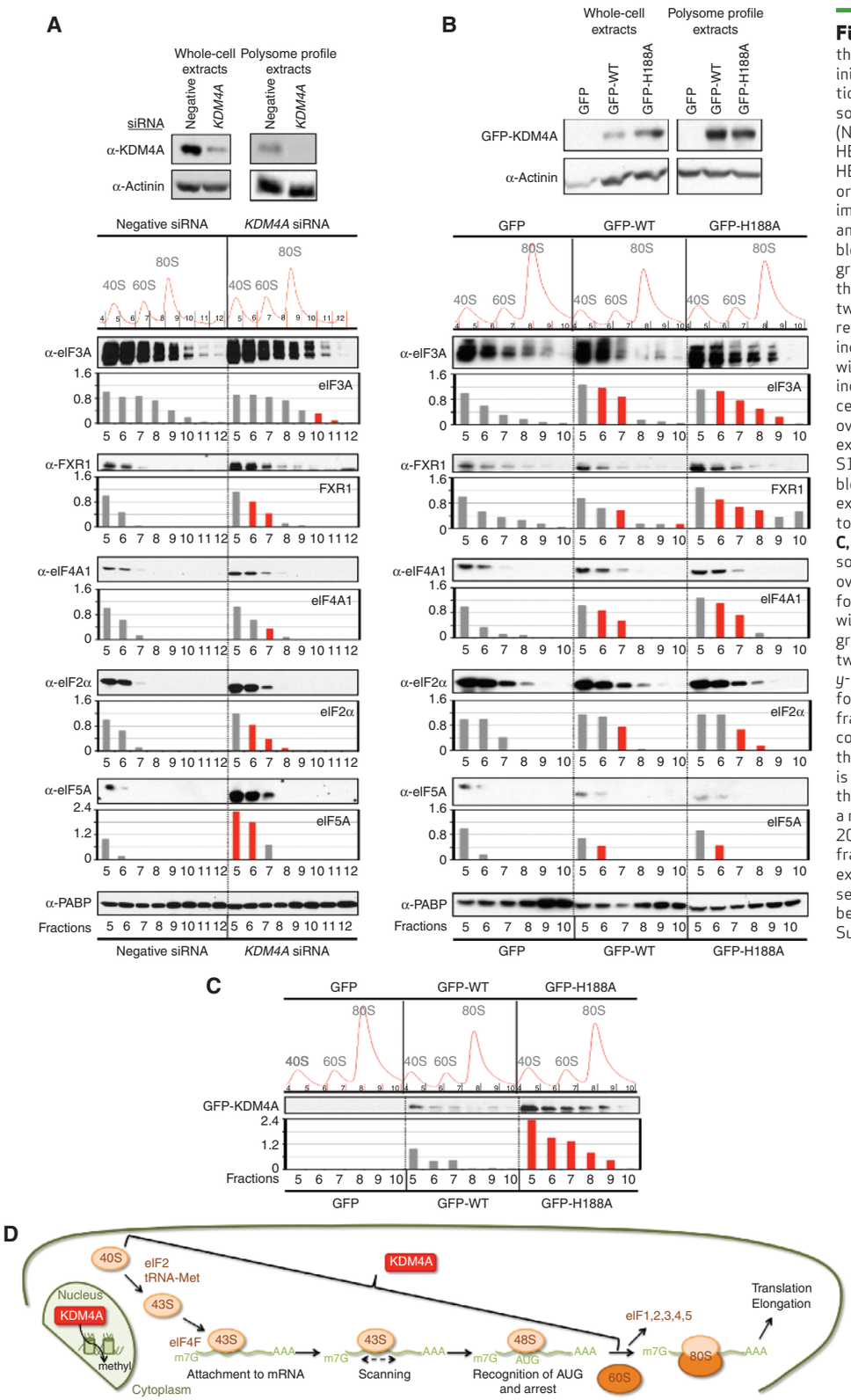

Figure 2. KDM4A levels affect the distribution of translation initiation factors. **A** and **B,** fractions collected from the polysome profiles [Negative Control (Negative) or KDM4A depleted HEK 293T cells for 48 hours (**A**); HEK 293T cells overexpressing WT or H188A for 24 hours (**B**)] were immunoblotted with the indicated antibodies. Representative Western blot analyses are shown below the graphs and represent the average of the quantification by ImageJ from two independent experiments. The red bars represent a reproducible increase of at least 20% compared with the control fractions from independent *KDM4A* siRNA–treated cells or KDM4A WT- or H188A-overexpressing cells (see individual experiments in Supplementary Fig. S1C and S1D). The top Western blot analysis represents whole cell extracts or the input extracts used to generate the polysome profiles. **C,** fractions collected from the polysome profiles from HEK 293T cells overexpressing GFP, WT, or H188A for 24 hours were immunoblotted with anti-GFP and the corresponding graph represents the average from two independent experiments. The *y*-axis represents the fold change for each fraction relative to the fraction five from the corresponding control. For **A,** the negative siRNA is the control, whereas for **B,** the GFP is the control. For **C,** the GFP-WT is the control. The red bars represent a reproducible increase of at least 20% compared with the GFP-WT fractions between two independent experiments. **D,** schematic representing where KDM4A could directly be involved in translation. Also see Supplementary Fig. S1.

Published OnlineFirst January 6, 2015; DOI: 10.1158/2159-8290.CD-14-1326

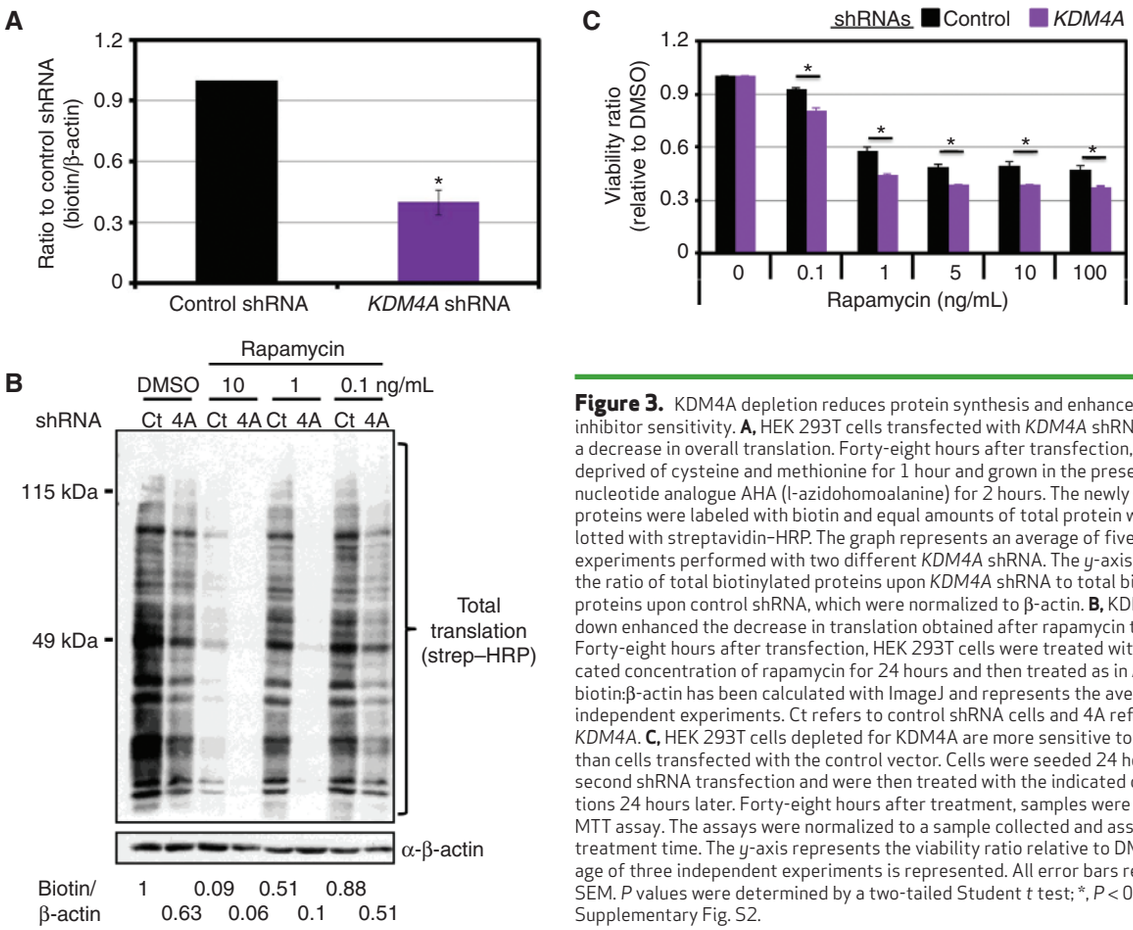

Figure 3. KDM4A depletion reduces protein synthesis and enhances mTOR inhibitor sensitivity. **A,** HEK 293T cells transfected with *KDM4A* shRNA present a decrease in overall translation. Forty-eight hours after transfection, cells were deprived of cysteine and methionine for 1 hour and grown in the presence of the nucleotide analogue AHA (l-azidohomoalanine) for 2 hours. The newly synthesized proteins were labeled with biotin and equal amounts of total protein were immunoblotted with streptavidin–HRP. The graph represents an average of five independent experiments performed with two different *KDM4A* shRNA. The *y*-axis represents the ratio of total biotinylated proteins upon *KDM4A* shRNA to total biotinylated proteins upon control shRNA, which were normalized to β-actin. **B,** KDM4A knockdown enhanced the decrease in translation obtained after rapamycin treatment. Forty-eight hours after transfection, HEK 293T cells were treated with the indicated concentration of rapamycin for 24 hours and then treated as in **A.** The ratio of biotin:β-actin has been calculated with ImageJ and represents the average of two independent experiments. Ct refers to control shRNA cells and 4A refers to shRNA *KDM4A*. **C,** HEK 293T cells depleted for KDM4A are more sensitive to rapamycin than cells transfected with the control vector. Cells were seeded 24 hours after the second shRNA transfection and were then treated with the indicated concentrations 24 hours later. Forty-eight hours after treatment, samples were analyzed by MTT assay. The assays were normalized to a sample collected and assayed at the treatment time. The *y*-axis represents the viability ratio relative to DMSO. The average of three independent experiments is represented. All error bars represent the SEM. *P* values were determined by a two-tailed Student *t* test; *, $P < 0.05$. Also see Supplementary Fig. S2.

and 1 ng/mL rapamycin coupled to KDM4A depletion resulted in approximately 50% and 90% reduction in protein synthesis, respectively (Fig. 3B; the biotin:β-actin ratio reported at the bottom represents the average of two independent experiments). These observations prompted us to assess the impact of KDM4A depletion on mTOR inhibitor sensitivity in cellular viability assays. As expected, KDM4A depletion coupled to rapamycin treatment resulted in a statistically significant decrease in cell viability across all drug doses (Fig. 3C). Consistent with these results, a polymorphism in *KDM4A* that results in reduced protein stability also confers sensitivity to mTOR inhibitors (14).

JmjC Demethylase Inhibition Causes Translation Initiation Defects

Previous studies report that KDM4A and KDM5A enzymes are chemical targets for JIB-04, an inhibitor of JmjC demethylases (15). Interestingly, KDM5A is enriched on genes involved in mTOR, p70S6K, and EIF2 signaling (16). In fact, KDM5A depletion reduced the expression of ribosomal protein genes (e.g., RPL3, RPL7, and RPL24; ref. 16). These observations are in contrast with KDM4A, as we did not observe significant alterations in gene expression for genes involved in translation or mTOR signaling, suggesting that these enzymes could cross-talk to translation machinery in different ways (Supplementary Fig. S3A). Consistent with KDM5A regulating mTOR and translation factor genes (16), we observed an increased sensitivity to rapamycin upon KDM5A depletion (Supplementary Fig. S3B and S3C), and a reduction in protein synthesis that was comparable to KDM4A depletion (Supplementary Fig. S3D). Because KDM4A was associated with the initiation complex, we also assessed whether KDM5A was present in the polysome fractions. Interestingly, KDM5A was present in the 40S and 60S fractions of polysome profiles (Supplementary Fig. S3E). These data suggest that KDM5A could regulate protein synthesis at the level of gene expression and translation complexes. Furthermore, they suggest that multiple KDMs could be involved in regulating protein synthesis and the response to drugs such as rapamycin. Therefore, we hypothesize that JIB-04 or related compounds could have a significant impact on sensitivity to mTOR inhibitors and protein synthesis by affecting both KDM4A and KDM5A or additional demethylases yet to be linked to protein synthesis.

To address this hypothesis, cells were cotreated with JIB-04 and rapamycin or AZD8055 (two different mTOR inhibitors) before proliferation and viability was assessed (Fig. 4A and B). JIB-04 treatment enhanced the effect of rapamycin and AZD8055 on both cell proliferation (Fig. 4A and Supplementary Fig. S3F) and viability (Fig. 4B). We further demonstrated this increased sensitivity to mTOR inhibitors in additional cancer

Published OnlineFirst January 6, 2015; DOI: 10.1158/2159-8290.CD-14-1326

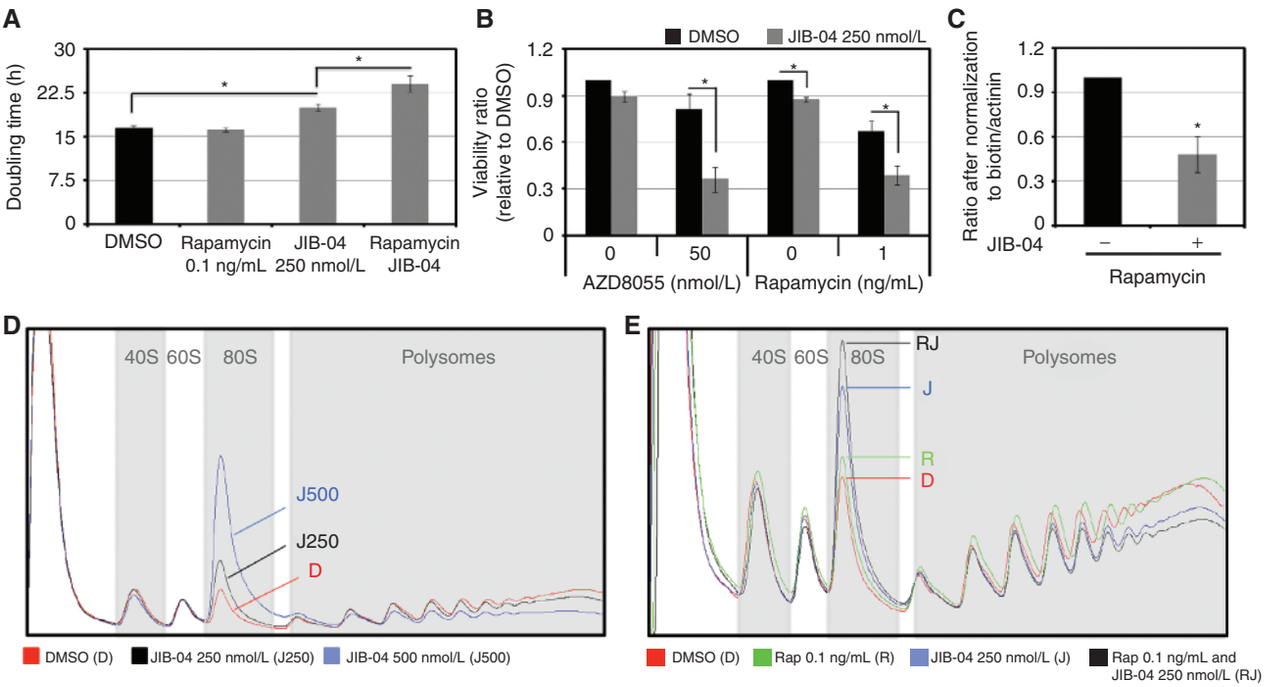

Figure 4. JIB-04 inhibits translation initiation. **A** and **B,** HEK 293T cells treated with JIB-04 are more sensitive to mTOR inhibitors than cells treated with vehicle. **A,** HEK 293T cells were treated with 250 nmol/L of JIB-04 and/or 0.1 ng/mL of rapamycin 24 hours after seeding. The *y*-axis represents the doubling time between 5 and 35 hours after rapamycin treatment. The average of three independent experiments is represented. **B,** HEK 293T cells were treated with the indicated drugs 24 hours after seeding, and 48 hours later they were analyzed by the MTT assay. The *y*-axis represents the viability ratio relative to DMSO. The average of three independent experiments is represented. **C,** JIB-04 enhanced the decrease in translation obtained after rapamycin treatment. HEK 293T cells were treated with 250 nmol/L of JIB-04 and/or 0.1 ng/mL of rapamycin for 24 hours and then treated as in Fig. 3A. The graph represents an average of three independent experiments. The *y*-axis represents the ratio after normalization to total biotinylated proteins to actinin. **D,** JIB-04–treated cells have a translation initiation defect. HEK 293T cells treated with the indicated concentration of JIB-04 for 24 hours before being analyzed by polysome profiling. **E,** JIB-04 enhanced the translation initiation defect obtained after rapamycin treatment. HEK 293T cells treated with 250 nmol/L of JIB-04 and/or 0.1 ng/mL of rapamycin for 24 hours were analyzed by polysome profiling. All error bars represent the SEM. *P* values were determined by a two-tailed Student *t* test; *, $P < 0.05$. Also see Supplementary Fig. S3.

cell lines (Supplementary Fig. S3G and S3H). Taken together, these data support the hypothesis that inactivation of KDM activity or reduced enzyme function could be used to sensitize cells to mTOR inhibition. We then tested whether JIB-04 altered overall translation and enhanced the translation defect observed with mTOR inhibitors. As expected, treatment with JIB-04 decreased overall protein synthesis (Supplementary Fig. S3I) and enhanced the translation defect observed upon rapamycin treatment (Fig. 4C and Supplementary Fig. S3I). Consistent with this defect, JIB-04 treatment resulted in a dose-dependent defect in translation initiation (Fig. 4D; increase of the 80S peak and decrease in polysomes). Furthermore, JIB-04 enhanced the initiation defect observed with different doses of rapamycin (Fig. 4E and Supplementary Fig. S3J). Taken together, these data highlight the impact that inhibition of KDM4-5 enzymes have on protein synthesis and demonstrate a new and unexpected involvement for JmjC enzymes in translation.

DISCUSSION

In this study, we assess the cytoplasmic role for KDM4A in protein synthesis. Altering the levels of KDM4A changed the distribution of translation initiation factors. This altered distribution could be due to the defective release of initiation factors because there was an accumulation of such factors in the 40S, 60S, and 80S fractions; however, KDM4A could also regulate additional events involved in translation or mRNA processing that could affect initiation and protein synthesis. Our data suggest that KDM4A directly affects initiation and protein synthesis because KDM4A interacts with the translation initiation machinery and is present in the initiating fractions of a polysome profile (i.e., 40S and 60S). Interestingly, there was more catalytically inactive KDM4A in the fractions where KDM4A is present. Therefore, catalytic activity appears to be important for properly regulating KDM4A distribution in these complexes, suggesting that components of the ribosome or ribosome-associated proteins are possible nonhistone substrates of KDM4A. However, our data also suggest that there could be a nonenzymatic function because overexpression of both catalytically active and inactive KDM4A affects the distribution of initiation factors. Therefore, future studies will be focused on understanding the enzymatic and nonenzymatic roles in modulating translation.

Our data demonstrate that reduced KDM4A levels are able to reduce overall protein synthesis without changing cell proliferation. However, the importance of this defect becomes enhanced with chemotherapeutics that target translation. The enhanced effect on translation inhibition correlates with a

Published OnlineFirst January 6, 2015; DOI: 10.1158/2159-8290.CD-14-1326

stronger decrease in cell proliferation. These observations are reminiscent of KDM4A depletion resulting in enhanced chemotherapeutic sensitivity to DNA replication drugs, which is another process directly regulated by KDM4A (7). Taken together, these data suggest that inhibition of KDM could potentiate the effect of mTOR inhibitors in the context of various cancer types. mTOR inhibition is a first-line therapy in the treatment of breast cancer and is being tested in ovarian cancer (17–19). This study, albeit limited to a few models, suggests that breast cancer cells (Supplementary Fig. S3B; ref. 20) and ovarian cancer cells (Supplementary Fig. S3C) might be sensitized by JIB-04 treatment in their response to mTOR inhibition. These data strongly support the combined use of these chemotherapeutics in other cancer cell types.

We also provide evidence that other KDMs, such as KDM5A, increase mTOR inhibitor sensitivity. Interestingly, Tzatsos and colleagues (16) demonstrated that KDM5A was enriched at target genes involved in protein synthesis and the mTOR pathway. Because we also observe an enrichment of KDM5A in polysome profile fractions, this enzyme may affect protein synthesis and mTOR inhibitor sensitivity at multiple steps. Resolving whether one or both aspects are important for the impact of KDM5A on protein synthesis will be important for future studies. Finally, these studies suggest that other enzymes (e.g., demethylases and methyltransferases) could be involved in pathways with cross-talk with translation or mTOR–PI3K signaling. Because many of these enzymes are altered in cancer (e.g., exhibit mutations, copy-number variation, or altered expression), they could act as additional biomarkers in treating cancer. Studies evaluating the *KDM4A* and *KDM5A* genetic and expression status in relation to treatment efficacy could allow for more refined patient stratification, especially in the context of mTOR inhibitors.

Overall, the data presented in this study highlight the importance of understanding the impact enzymes have inside and outside the nucleus and of identifying the cross-talk between pathways for chemotherapeutics and chromatin regulators. The discovery that KDM4A or KDM5A depletion results in a decrease in protein synthesis suggests that there is a benefit in targeting this group collectively. Therefore, the lack of currently available KDM-specific inhibitors could be balanced by the benefit of targeting groups of KDMs, especially in combined therapy. This strategy is currently being applied for histone deacetylase (21). The combined targeting of KDMs and translation could result in an effective therapy with reduced single-agent toxicity, while providing the advantage of reducing the emergence of resistant clones because both KDM4A and KDM5A have been linked to mechanisms that could promote resistance (8, 22). These possibilities are important areas to explore in the future. Finally, the current study highlights the fact that discovering unappreciated functions for chromatin modifiers can lead to the identification of associated signaling pathways and uncover optimal chemotherapeutic targets for the future.

METHODS

Cell Culture and Drug Treatments

For tissue culture procedures, see ref. 7. Rapamycin (LC Laboratories) and AZD8055 (Selleckchem) were used at indicated concentrations. JIB-04 (Xcessbio) was used at a final concentration of 250 or 500 nmol/L, as annotated. For the translation assays, DMEM depleted of methionine and cysteine (Life Technologies; 21013-024) was used. HEK 293T cells have been obtained from the ATCC; no authentication has been done by the authors.

Plasmids, siRNAs, and Transfections

Plasmid transfections were performed using X-tremeGENE 9 DNA transfection reagent (Roche) on 6×10^5 HEK 293T cells plated in 10-cm dishes 20 hours before transfection. The complexes were incubated with the cells in OptiMEM for 4 hours before being replaced by fresh media. The transfected plasmids were pMSCV-GFP (7), pMSCV-GFP-KDM4A (7), pMSCV-GFP-KDM4A-H188A (7), pSUPER (7), pSUPER-4C (referred as 4A.2 throughout the figures; ref. 7), pLKO, pLKO-A06 (referred as 4A.6 throughout the figures), and pLKO-A10 (referred as 4A.10 throughout the figures). For the MTT assays, shRNAs were transfected twice 48 hours apart. siRNA transfections were performed using X-tremeGENE siRNA transfection reagent (Roche) or Lipofectamine 3000 (Life Technologies) following vendors' instructions. The transfected siRNAs were Silencer Select (Life Technologies) *KDM4A* (s18636 and s18637), *KDM5A* (s11834 and s11836), and negative control #1.

Western Blot Analysis

Western blot analyses were performed as described previously (7).

Cell Fractionation

Cytoplasmic, nuclear, and chromatin fractions were prepared from RPE cells. Cell pellets were washed twice in ice-cold PBS and resuspended in ice-cold Buffer A (10 mmol/L HEPES pH 7.9, 10 mmol/L KCl, 0.1 mol/L EDTA, and 0.5 mol/L EGTA) and incubated on ice for 15 minutes. Swollen cells were lysed by the addition of NP-40 to 0.8% with 10 seconds of vortexing.

Lysed cells were centrifuged, and the supernatant kept as the cytoplasmic extract. The nuclear pellet was resuspended in Buffer C (10 mmol/L HEPES pH 7.9, 400 mmol/L NaCl, 1 mmol/L EDTA, and 5 mmol/L EGTA), dounced to resuspend, and incubated at 4°C for 30 minutes with rotation. Extracts were centrifuged, and the supernatant kept as nuclear extract. Chromatin pellets were resuspended in N-Buffer (20 mmol/L Tris pH 7.5, 100 mmol/L KCl, 2 mmol/L $MgCl_2$, 1 mmol/L $CaCl_2$, 0.3 mol/L sucrose, 0.1% Triton X-100, and 3 U/mL micrococcal nuclease). Samples were sonicated for 10 minutes at 70% amplitude in a Q700 cup horn and then incubated at room temperature for 15 minutes for MNase digestion. Reactions were stopped by the addition of 5 mmol/L EGTA and centrifuged to clear. Supernatant was kept as chromatin extract. For the Western blot analysis, a comparable fraction of each compartment was loaded on a gel. The Western blot analysis depicted in Fig. 1A was compiled from nonadjacent images from the same exposure of the same blot.

Antibodies

The antibodies used were LDH (Santa Cruz Biotechnology, sc-133123), Histone H3 (Abcam; ab1791), actinin (Santa Cruz Biotechnology; sc-17829), streptavidin–HRP (Cell Signaling Technology; 3999S), eIF3A (Abcam; ab118357), eIF4A1 (Abcam; ab31217), FXR1 (Abcam; ab129089), PABP (Abcam; ab21060), eIF5A (Abcam; ab32443), eIF2α (Invitrogen; AH00802), eIF4G1 (Abcam; ab2609), p53 (Santa-Cruz; sc-126 X), eIF4A3 (Abcam; ab32485), eIF4E (Cell Signaling Technology; 20675), RPS6 (Abcam; ab58350), eIF3D (Abcam; ab12442), S6K1 (Abcam; ab32529), S6K1pT389 (Abcam; ab2571), RPS6pS235 (Abcam; ab12864), and KDM5A (Abcam; ab70892). KDM4A and β-actin antibodies were described previously (23). MCM7 antibody was described previously (8). KDM4A immunoprecipitations were performed with KDM4A-P006.

Published OnlineFirst January 6, 2015; DOI: 10.1158/2159-8290.CD-14-1326

Coimmunoprecipitation

The coimmunoprecipitations experiments were performed as described previously (23).

Mass Spectrometry Analysis on KDM4A Immunoprecipitations

Mass spectrometry analysis were performed as described previously (8).

Multiplexed Quantitative Proteomics

Multiplexed quantitative proteomics using tandem mass tag reagents (TMT; Thermo Scientific) and a synchronous precursor selection-based MS3 method (11) on an Orbitrap Fusion mass spectrometer (Thermo Scientific). For a complete methods protocol, see Supplementary Experimental Procedures.

Monitored Cell Proliferation Assay

Twenty-four hours after transfection, 1×10^4 HEK 293T cells per well were seeded on a 96-well plate, and then treated after 24 hours. Cell proliferation was monitored with an xCELLigence system (Roche; ref. 24).

MTT Assays

MTT assays were performed following the supplier's instructions from the Cell Proliferation Kit I (MTT) from Roche. For shRNA experiments, after two subsequent shRNA transfections, 1×10^4 cells were seeded in 96-well plates 24 hours before treatment. Forty-eight hours later, cells were assayed. We determined sensitivity by subtracting the background from the absorbance.

Translation Assays

Translation assays were performed following the supplier's instructions from Click-IT Metabolic Labeling Reagents for Proteins (Life Technologies). Cells were incubated in the presence of DMEM without cysteine and methionine for 1 hour, then grown in the presence of 50 μmol/L AHA (l-azidohomoalanine; Life Technologies C10102) for 2 hours, harvested, and washed extensively with PBS. Cells were lysed in 1% SDS in 50 mmol/L Tris pH 8.0 with 10% glycerol and sonicated using a bath sonicator (QSonica Q700) for 30 minutes. The Click-IT reactions were performed following the supplier's instructions from Click-IT Protein Reaction Buffer Kit (Life Technologies). Briefly, 50 to 100 μg of lysates were used per reaction with 40 μmol/L Alkyne-Biotin (Life Technologies; B10185), and 10 μg were assayed by Western blot analysis using a Streptavidin antibody conjugated to horseradish peroxidase (HRP).

Polysome Profiling

HEK 293T cells were grown to 80% confluence in 10-cm^2 plates. Cells were washed and scraped into 100 μg/mL cycloheximide/PBS. Cells were pelleted and resuspended in 300 to 500 μL polysome lysis buffer (5 mmol/L Tris pH 7.4, 2.4 mmol/L $MgCl_2$, and 1.5 mmol/L KCl), freshly supplemented with 10 μg/mL cyclohexamide, 2 μmol/L DTT, 0.5% Triton-X, 0.5% sodium deoxycholate, and protease and phosphatase inhibitors. Lysis buffer volume was adjusted for cell number. Lysates were cleared for 10 minutes at 18,000 × *g*, and 4°C. Cleared lysates (250 μL) were loaded onto 12-mL 10% to 50% sucrose gradients (prepared in 15 mmol/L Tris pH 7.4, 15 mmol/L $MgCl_2$, and 150 mmol/L NaCl) and spun for 2 hours in a SW40Ti rotor (Beckman Coulter), at 40,000 rpm and 4°C. Immediately following centrifugation, 0.5-mL fractions were collected using a BioComp Gradient Master instrument. For Western blot analysis, 200 μL of each fraction were precipitated by methanol/chloroform extraction and loaded on a gel.

Microarrays Analysis

For RNA expression analysis, RNA was extracted using the MiRNeasy Mini kit (Qiagen). cDNA synthesis was performed with 2 μg of total RNA using the Roche cDNA synthesis System (11 117 831 001; Roche). Hybridization of cDNA to Human Gene Expression 12 × 135 K Arrays (Roche Nimblegen) was performed in triplicate according to the manufacturer's protocol. Arrays were scanned using MS200 scanner (Roche Nimblegen) and extracted using Roche DEVA software. Raw expression array data were RMA normalized and $\log_2$ transformed. Differential expression *t* tests were computed using the empirical Bayes shrinkage procedure implemented in the Limma R/Bioconductor package (25). Two-fold upregulated or downregulated genes with a $P < 0.05$ were considered differentially regulated. The accession number for the microarray analysis is GSE63812.

Statistical Analysis

All errors bars represent SEM. *P* values were determined by a two-tailed Student *t* test; the asterisk (*) represents $P < 0.05$.

Disclosure of Potential Conflicts of Interest

J.R. Whetstine is a consultant/advisory board member for Qsonica. No potential conflicts of interest were disclosed by the other authors.

Authors' Contributions

Conception and design: C. Van Rechem, J.R. Whetstine
Development of methodology: C. Van Rechem
Acquisition of data (provided animals, acquired and managed patients, provided facilities, etc.): C. Van Rechem, J.C. Black, M. Boukhali, C.H. Benes
Analysis and interpretation of data (e.g., statistical analysis, biostatistics, computational analysis): C. Van Rechem, J.C. Black, M.J. Aryee, W. Haas, C.H. Benes, J.R. Whetstine
Writing, review, and/or revision of the manuscript: C. Van Rechem, C.H. Benes, J.R. Whetstine
Administrative, technical, or material support (i.e., reporting or organizing data, constructing databases): S. Gräslund, J.R. Whetstine
Study supervision: J.R. Whetstine
Other (carried out TMT mass spectrometry experiment): M. Boukhali

Acknowledgments

The authors thank Drs. Cailin Joyce and Carl Novina for providing access to the BioComp Gradient Master instrument as well as training. The authors also thank Drs. Mo Motamedi, Elnaz Atabakhsh, and Sweta Mishra, as well as Kelly Biette, for their comments and suggestions. The authors thank Tony Kossiakoff, Edyta Marcon, Cheryl Arrowsmith, and members of the Structural Genomics Consortium (SGC) Antibody team for contributions to generating recombinant KDM4A-P006.

Grant Support

The studies conducted in this article were funded by the following: the American Cancer Society Basic Scholar Grant, the Massachusetts General Hospital (MGH) Proton Beam Federal Share Grant (CA059267), and NIH R01GM097360 to J.R. Whetstine; and NIH U54 HG006097 to C.H. Benes. J.R. Whetstine is the Tepper Family MGH Research Scholar and a Leukemia and Lymphoma Society Scholar, as well as a recipient of the American Lung Association Lung Cancer Discovery Award. A postdoctoral fellowship was provided by the Fund for Medical Discovery to C. Van Rechem. C. Van Rechem is the 2014 Skacel Family Marsha Rivkin Center for Ovarian Cancer Research Scholar. This research was supported, in part, by a grant from the Marsha Rivkin Center for Ovarian Cancer Research.

Published OnlineFirst January 6, 2015; DOI: 10.1158/2159-8290.CD-14-1326

J.C. Black was a Fellow of The Jane Coffin Childs Memorial Fund for Medical Research and is supported by the MGH ECOR Tosteson Postdoctoral Fellowship. This investigation has been aided by a grant from The Jane Coffin Childs Memorial Fund for Medical Research. The SGC is a registered charity (no. 1097737) that receives funds from AbbVie, Boehringer Ingelheim, the Canada Foundation for Innovation (CFI), the Canadian Institutes of Health Research (CIHR), Genome Canada, Ontario Genomics Institute Grant OGI-055, GlaxoSmithKline, Janssen, Lilly Canada, the Novartis Research Foundation, the Ontario Ministry of Economic Development and Innovation, Pfizer, Takeda, and Wellcome Trust Grant 092809/Z/10/Z. Work in the Kossiakoff laboratory was funded by the SGC and the NIH.

The costs of publication of this article were defrayed in part by the payment of page charges. This article must therefore be hereby marked *advertisement* in accordance with 18 U.S.C. Section 1734 solely to indicate this fact.

Received November 10, 2014; revised December 8, 2014; accepted December 19, 2014; published OnlineFirs; January 6, 2015.

REFERENCES

1. Mazur PK, Reynoird N, Khatri P, Jansen PW, Wilkinson AW, Liu S, et al. SMYD3 links lysine methylation of MAP3K2 to Ras-driven cancer. Nature 2014;510:283–7.
2. Su IH, Dobenecker MW, Dickinson E, Oser M, Basavaraj A, Marqueron R, et al. Polycomb group protein ezh2 controls actin polymerization and cell signaling. Cell 2005;121:425–36.
3. Donlin LT, Andresen C, Just S, Rudensky E, Pappas CT, Kruger M, et al. Smyd2 controls cytoplasmic lysine methylation of Hsp90 and myofilament organization. Genes Dev 2012;26:114–9.
4. Van Rechem C, Whetstine JR. Examining the impact of gene variants on histone lysine methylation. Biochim Biophys Acta 2014;1839: 1463–76.
5. Greer EL, Shi Y. Histone methylation: a dynamic mark in health, disease and inheritance. Nat Rev Genet 2012;13:343–57.
6. Black JC, Van Rechem C, Whetstine JR. Histone lysine methylation dynamics: establishment, regulation, and biological impact. Mol Cell 2012;48:491–507.
7. Black JC, Allen A, Van Rechem C, Forbes E, Longworth M, Tschop K, et al. Conserved antagonism between JMJD2A/KDM4A and HP1gamma during cell cycle progression. Mol Cell 2010;40:736–48.
8. Black JC, Manning AL, Van Rechem C, Kim J, Ladd B, Cho J, et al. KDM4A lysine demethylase induces site-specific copy gain and rereplication of regions amplified in tumors. Cell 2013;154:541–55.
9. Berry WL, Janknecht R. KDM4/JMJD2 histone demethylases: epigenetic regulators in cancer cells. Cancer Res 2013;73:2936–42.
10. Kim TD, Shin S, Berry WL, Oh S, Janknecht R. The JMJD2A demethylase regulates apoptosis and proliferation in colon cancer cells. J Cell Biochem 2012;113:1368–76.
11. Ting L, Rad R, Gygi SP, Haas W. MS3 eliminates ratio distortion in isobaric multiplexed quantitative proteomics. Nat Methods 2011; 8:937–40.
12. Bjornsti MA, Houghton PJ. The TOR pathway: a target for cancer therapy. Nat Rev Cancer 2004;4:335–48.
13. Populo H, Lopes JM, Soares P. The mTOR signalling pathway in human cancer. Int J Mol Sci 2012;13:1886–918.
14. Van Rechem C, Black JC, Greninger P, Zhao Y, Donado C, Burrowes PD, et al. A coding single-nucleotide polymorphism in lysine demethylase *KDM4A* associates with increased sensitivity to mTOR inhibitors. Cancer Discov 2015;5:245–54.
15. Wang L, Chang J, Varghese D, Dellinger M, Kumar S, Best AM, et al. A small molecule modulates Jumonji histone demethylase activity and selectively inhibits cancer growth. Nat Commun 2013;4:2035.
16. Tzatsos A, Paskaleva P, Ferrari F, Deshpande V, Stoykova S, Contino G, et al. KDM2B promotes pancreatic cancer via Polycomb-dependent and -independent transcriptional programs. J Clin Invest 2013;123:727–39.
17. Ciruelos Gil EM. Targeting the PI3K/AKT/mTOR pathway in estrogen receptor–positive breast cancer. Cancer Treat Rev 2014;40: 862–71.
18. Jerusalem G, Rorive A, Collignon J. Use of mTOR inhibitors in the treatment of breast cancer: an evaluation of factors that influence patient outcomes. Breast Cancer 2014;6:43–57.
19. Mabuchi S, Hisamatsu T, Kimura T. Targeting mTOR signaling pathway in ovarian cancer. Curr Med Chem 2011;18:2960–8.
20. Roberts PJ, Usary JE, Darr DB, Dillon PM, Pfefferle AD, Whittle MC, et al. Combined PI3K/mTOR and MEK inhibition provides broad antitumor activity in faithful murine cancer models. Clin Cancer Res 2012;18:5290–303.
21. Bots M, Johnstone RW. Rational combinations using HDAC inhibitors. Clin Cancer Res 2009;15:3970–7.
22. Sharma SV, Lee DY, Li B, Quinlan MP, Takahashi F, Maheswaran S, et al. A chromatin-mediated reversible drug-tolerant state in cancer cell subpopulations. Cell 2010;141:69–80.
23. Van Rechem C, Black JC, Abbas T, Allen A, Rinehart CA, Yuan GC, et al. The SKP1-Cul1-F-box and leucine-rich repeat protein 4 (SCF-FbxL4) ubiquitin ligase regulates lysine demethylase 4A (KDM4A)/Jumonji domain-containing 2A (JMJD2A) protein. J Biol Chem 2011;286:30462–70.
24. Vistejnova L, Dvorakova J, Hasova M, Muthny T, Velebny V, Soucek K, et al. The comparison of impedance-based method of cell proliferation monitoring with commonly used metabolic-based techniques. Neuro Endocrinol Lett 2009;30(suppl 1):121–7.
25. Bioinformatics and computational biology solutions using R and bioconductor.Gentleman R, Carey V, Huber W, Dudoit S, Irizarry R, editors. New York: Springer; 2005. p. 397–420.

Published OnlineFirst January 6, 2015; DOI: 10.1158/2159-8290.CD-14-1326

AACR American Association for Cancer Research

CANCER DISCOVERY

Lysine Demethylase KDM4A Associates with Translation Machinery and Regulates Protein Synthesis

Capucine Van Rechem, Joshua C. Black, Myriam Boukhali, et al.

Cancer Discovery 2015;5:255-263. Published OnlineFirst January 6, 2015.